# Identity-specific coding of future rewards in the human orbitofrontal cortex

James D. Howard[a], Jay A. Gottfried[a], Philippe N. Tobler[b], and Thorsten Kahnt[a,1]

[a]Department of Neurology, Northwestern University Feinberg School of Medicine, Chicago, IL 60611; and [b]Department of Economics, University of Zurich, Zurich 8006, Switzerland

Edited by Ranulfo Romo, Universidad Nacional Autonóma de México, Mexico City, D.F., Mexico, and approved March 16, 2015 (received for review February 19, 2015)

**Nervous systems must encode information about the identity of expected outcomes to make adaptive decisions. However, the neural mechanisms underlying identity-specific value signaling remain poorly understood. By manipulating the value and identity of appetizing food odors in a pattern-based imaging paradigm of human classical conditioning, we were able to identify dissociable predictive representations of identity-specific reward in orbitofrontal cortex (OFC) and identity-general reward in ventromedial prefrontal cortex (vmPFC). Reward-related functional coupling between OFC and olfactory (piriform) cortex and between vmPFC and amygdala revealed parallel pathways that support identity-specific and -general predictive signaling. The demonstration of identity-specific value representations in OFC highlights a role for this region in model-based behavior and reveals mechanisms by which appetitive behavior can go awry.**

reward value | associative learning | ventromedial prefrontal cortex | olfaction | multivoxel pattern analysis

Predictive representations of future outcomes are critical for guiding adaptive behavior. To choose different types of rewards, such as food, shelter, and mates, it is essential that predictive signals contain specific information about the identity of those outcomes. Food rewards differ dramatically in their nutritional composition, and identity-specific cues allow differential foraging depending on current needs of the organism. The absence of precise mappings between predictive reward signals and their intended outcomes would have devastating effects on food-based decisions.

Despite the ecological relevance of outcome-specific predictive coding, which can be observed even in *Drosophila* (1), most research in human and nonhuman primates has focused on "common currency" signals of economic values in the orbitofrontal cortex (OFC) (2, 3) and ventromedial prefrontal cortex (vmPFC) (4–8). These signals, which by definition are independent of the specific nature of the reward, can be used to compare and choose between alternative outcomes, but are unable to inform expectations about the specific identity of the outcome. For this, identity-specific representations that conjointly represent information about both affective value (how good is it?) and outcome identity (what is it?) are necessary. Recent data suggest that the OFC is involved in signaling information about specific outcomes (9–14). For instance, many OFC neurons signal both the value and the identity of the predicted outcome (12), and OFC lesions diminish the effects of outcome identity (but not general affective value) on conditioned behavior (13).

Recent imaging work has also begun to address how the human brain encodes predictive information about rewarding outcomes. One study (9) used a functional magnetic resonance imaging (fMRI) adaptation paradigm to provide evidence for identity-based codes for reward in the OFC. Another investigation (4) used fMRI data from a willingness to pay auction combined with decoding techniques to reveal category-dependent and -independent value codes in vmPFC and lateral OFC, respectively. However, neither of these studies varied value independently of identity, and they were therefore unable to test for the presence of identity-specific and -general value codes in the OFC.

Here, we combined an olfactory paradigm of classical conditioning with fMRI pattern-based approaches to test the hypothesis that the human OFC simultaneously encodes both the value and the identity of an expected rewarding outcome. Critically, we took advantage of two unique properties of appetizing food odors to reveal identity-specific value representations. First, food odors act as potent rewards (15–17), with pleasantness that can scale with odor intensity (18, 19). Second, different food odors vary widely in identity (e.g., chocolate cake vs. pizza) but may still hold similar value. These distinct features enabled us to systematically manipulate outcome value and identity independently within the same stimulus space.

## Results

**Behavior.** One day before fMRI scanning, hungry subjects ($n$ = 15) (Fig. 1*A*) rated the pleasantness of eight food odors, including four sweet odors (cupcake, strawberry, dulce de leche, and watermelon) and four savory odors (pizza, sautéed onions, potato chips, and barbecue sauce) (Fig. 1*B*). Based on each subject's ratings, we selected one sweet odor and one savory odor that were matched in rated pleasantness. Next, for each subject, low- (corresponding to low-value stimuli) and high-intensity (corresponding to high-value stimuli) versions of these two odors were created by adjusting stimulus concentrations through an olfactometer (*SI Materials and Methods* and *SI Discussion*). This procedure resulted in a final selection of four odors, comprising a fully balanced two-factorial design (two identity levels by two

### Significance

**To make adaptive choices based on reward-predicting stimuli, organisms must take into account information about both the value and the specific identity of the reward to be obtained. Using appetizing food odors and pattern-based functional magnetic resonance imaging, we show that the human orbitofrontal cortex encodes future rewards in the form of identity-specific value codes. That is, even if valued the same, different expected rewards, such as pizza and chocolate cake, are differently encoded in this region. We further show that identity-specific and -general value coding regions are functionally linked to distinct regions, providing a novel account for the neural circuitry that underlies integration of both sensory and affective information to guide reward-related behavior.**

Author contributions: J.D.H., J.A.G., P.N.T., and T.K. designed research; J.D.H. and T.K. performed research; T.K. analyzed data; and J.D.H., J.A.G., P.N.T., and T.K. wrote the paper.

The authors declare no conflict of interest.

This article is a PNAS Direct Submission.

[1]To whom correspondence should be addressed. Email: thorsten.kahnt@northwestern.edu.

This article contains supporting information online at www.pnas.org/lookup/suppl/doi:10.1073/pnas.1503550112/-/DCSupplemental.

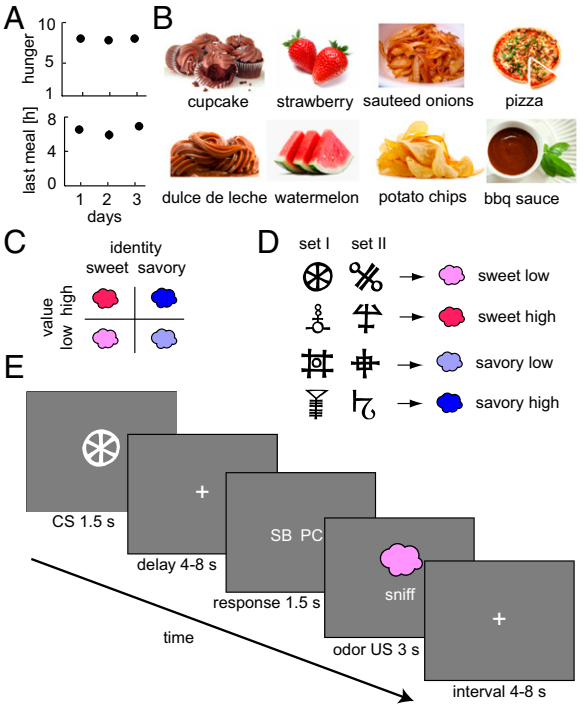


**Fig. 1.** Experimental design and stimuli. (*A*, *Upper*) Hunger ratings and (*A*, *Lower*) time to last meal did not differ across days (one-way ANOVAs: hunger, $F_{2,28} = 0.34$, $P = 0.71$; time to last meal, $F_{2,28} = 0.97$, $P = 0.39$). Note that error bars for SEM ($n = 15$) are smaller than the symbols. (*B*) Pictorial representations of the sweet and savory food odor stimuli used in the experiment. (*C*) Illustration of the two-factorial design of our study, in which value (low vs. high) and identity (sweet vs. savory) could be independently manipulated. (*D*) Subjects learned to associate each of four odor US with two unique visual CS, resulting in two stimulus sets (counterbalanced across subjects). (*E*) On each trial of the fMRI task, one of eight CS images was presented, and subjects had to predict either the value of the upcoming US [response options: low (L) and high (H)] or the identity of the upcoming US [response options in this example: strawberry (SB) and potato chips (PC)]. This prediction was followed by a sniff cue and delivery of odor.

value levels) (Fig. 1*C*). These odors were then used as unconditioned stimuli (US) in a classical conditioning procedure on the first day of the experiment, wherein each odor was paired with two unique visual conditioned stimuli (CS) (Fig. 1*D*).

Subjects underwent fMRI scanning on the next 2 days of the study while again receiving the same CS–US pairings (Fig. 1*D*). Pleasantness ratings obtained on both scanning days confirmed the efficacy of our odor intensity manipulation, whereby the two odor identities (sweet and savory) were matched in value for both low- and high-intensity levels. A two-way repeated measures ANOVA ($n = 15$) revealed a significant main effect of value ($F_{1,14} = 33.48$, $P < 0.001$) in the absence of a main effect of identity ($F_{1,14} = 0.36$, $P = 0.56$) or a value by identity interaction ($F_{1,14} = 0.02$, $P = 0.91$) (Fig. 2*A*). This profile was also found for CS pleasantness ratings, indicating that the CS images acquired predictive value information about their associated odor outcomes (two-way repeated measures ANOVA, $n = 15$; main effect of value: $F_{1,14} = 28.86$, $P < 0.001$; main effect of identity: $F_{1,14} = 0.03$, $P = 0.86$; interaction: $F_{1,14} = 0.001$, $P = 0.97$) (Fig. 2*B* and Fig. S1, individual data). A similar effect was observed in the sniffing responses (sniff amplitude) (Fig. 2 *C* and *D*), which differed as a function of odor value (two-way repeated measures ANOVA, $n = 15$; $F_{1,14} = 9.05$, $P = 0.01$) but not identity ($F_{1,14} = 3.60$, $P = 0.08$). Although there were small but significant differences between low- and high-value sniffs (percentage change from low to high: 3.95% and 5.24% for sweet and savory, respectively), there was no significant interaction ($F_{1,14} = 0.14$, $P = 0.71$), indicating that any comparisons between sweet and savory value effects could not be explained by respiratory differences per se. Moreover, all fMRI analyses focused on the CS presentations, which were temporally dissociated from the odor presentations, and for which no differences in respiration were observed (two-way repeated measures ANOVA, $n = 15$; main effect of value: $F_{1,14} = 0.09$, $P = 0.76$; main effect of identity: $F_{1,14} = 0.02$, $P = 0.89$; interaction: $F_{1,14} = 0.47$, $P = 0.50$). Nevertheless, to comprehensively control for any potential breathing-related effects, sniff parameters were included in all fMRI models (20). Fig. S2 shows additional analyses on behavioral task performance.

**Identity-Specific Value Codes in OFC.** The ability to modulate predictive value while "clamping" predictive identity motivated our next efforts to isolate CS-evoked fMRI representations of identity-specific value. We reasoned that if expected value codes contain identity information, then value-related (high vs. low value) patterns of fMRI ensemble activity corresponding to the different outcome identities (sweet vs. savory) should be reliably distinguishable. Using a multivoxel pattern-based searchlight analysis (21), we first computed the value-related response patterns during CS presentation (high minus low value) separately for sweet- and savory-predictive CS cues (Fig. 3*A*). In a second step, we used cross-validated support vector machines (SVMs) to identify regions in which these value-related response patterns—corresponding to different predicted outcome identities—could be reliably classified (Fig. 3*A*), the idea being that significant decoding accuracy would be observed only if the value-related activity patterns for the two predicted odors are different. We identified robust codes of identity-specific value in three brain areas: lateral OFC [$x, y, z$ coordinates = 42, 36, −16; $t$ test, $n = 15$; $t = 5.72$, $p$ familywise error rate ($p_{FWE}$) = 0.022] (Fig. 3*B*), anterior cingulate cortex (ACC; 6, 38, 16; $t = 5.01$, $p_{FWE} = 0.038$) (Fig. 3*C*), and hippocampus (38, −16, −16; $t = 4.92$, $p_{FWE} = 0.020$). The cluster in the lateral OFC was located in Brodmann area 47, roughly corresponding to areas 47/12m and 47/12r in the classification from ref. 22 and areas 47/12m and 47/12o in the classification from ref. 23.

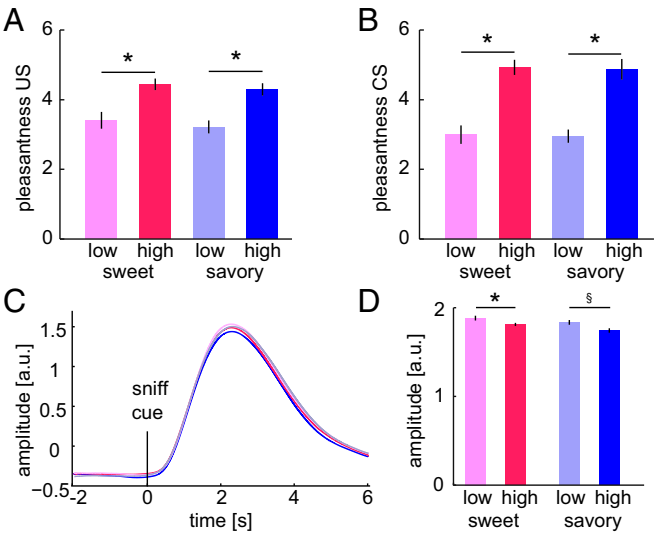


**Fig. 2.** Pleasantness ratings and breathing data. (*A* and *B*) Pleasantness ratings of (*A*) US and (*B*) CS were systematically higher for high- vs. low-intensity stimuli (paired $t$ tests). (*C*) Average sniff responses locked to the sniff cue. (*D*) Average peak sniff amplitudes. Error bars are SEMs ($n = 15$). $t$ test ($n = 15$). $^*P < 0.05$; $^{\S}P = 0.052$.

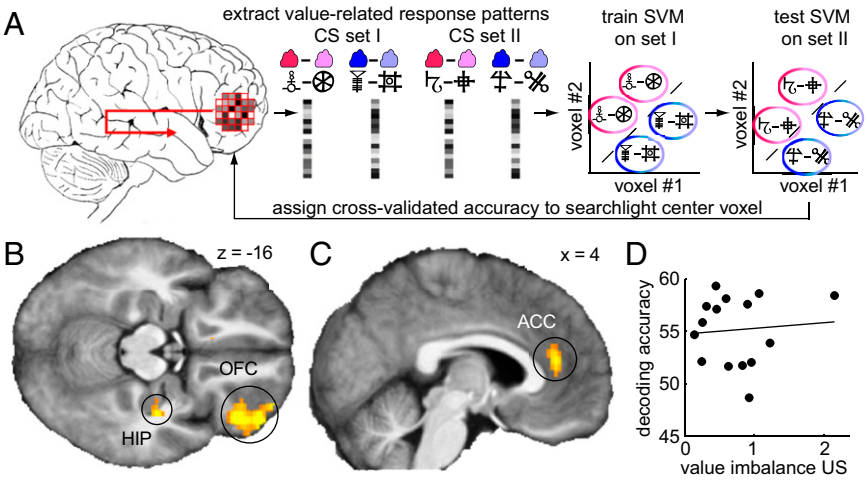


**Fig. 3.** OFC represents identity-specific predictive values. (*A*) Schematic of the searchlight decoding analysis used to reveal identity-specific value codes. Value-related voxel responses (i.e., fMRI signal difference between high- and low-value conditions) were extracted for CS images predicting sweet odors (pink/red colors) and savory odors (blue colors). An SVM was trained to classify the identity of value-related (high vs. low value) response patterns for one set of CS and then, tested on the second set of CS (to ensure that effects were not driven by mere visual features of the CS images). (*B* and *C*) Identity-specific value responses were identified in OFC, hippocampus (HIP), and ACC. Display threshold is $P < 0.001$. (*D*) Value imbalances between sweet and savory odors have no impact on identity-specific coding ($r = 0.08$, $P = 0.76$), suggesting that decoding is not based on residual value differences between the two odor identities.

Although these findings suggest that the brain encodes predictive values intrinsically linked to specific outcome identities, it is possible that imperfect balancing of relative value (high vs. low) between the sweet and savory odors within individual subjects could have led to spurious decoding. For example, if the sweet-predictive high- vs. low-reward CS was perceived to be more rewarding than the savory-predictive high- vs. low-reward CS, then value differences (rather than identity differences alone) could have influenced the observed classification effects. To rule out this potential confound, we tested the correlation between decoding accuracy and a measure of value imbalance, which compares the difference in value between low- and high-value levels between the two odors (basically, the difference of the differences) (*SI Materials and Methods*). Supporting the notion that decoding was, indeed, based on identity-specific value patterns, the correlations between value imbalance and decoding accuracy were nonsignificant in OFC ($r = 0.08$, $P = 0.76$) (Fig. 3*D*), ACC ($r = -0.27$, $P = 0.32$), and hippocampus ($r = -0.12$, $P = 0.66$).

**Identity-General Value Codes in vmPFC.** Although we found evidence for identity-specific value codes in the OFC, it remains possible that predictive representations of identity-general value may be encoded elsewhere. We hypothesized that, in this instance, value signals would generalize from one odor identity to the other. Thus, by training an SVM on activity patterns from CS images predicting the value of sweet odors (high vs. low value), we should be able to correctly classify activity patterns from CS cues predicting the value of savory odors and vice versa (Fig. 4*A*). Using this approach, we found significant decoding of general value signals in vmPFC (−8, 38, −10; *t* test, $n = 15$; $t = 5.19$, $p_{FWE} = 0.03$) (Fig. 4*B*). Notably, this relatively small cluster in medial Brodmann area 11 (corresponding to area 10m/10r in ref. 22 and area 14m in ref. 23) closely colocalizes with coordinates ($x = -7$, $y = 38$, $z = -11$) from previous fMRI studies of "common value" (8). To confirm that these findings reflect identity-general value coding, we predicted that greater value mismatch between sweet and savory odors would weaken classification performance. Results show that greater value imbalance between odor identities was correlated with lower decoding accuracy in vmPFC ($r = -0.68$, $P = 0.01$) (Fig. 4*C*), providing additional evidence that this region supports value coding independent of reward identity.

**Independent Pathways for Identity-Specific and -General Values.** We next tested whether identity-specific and -general predictive value signals are part of a serial network or whether they reflect independent processes. In the former scenario, general value would be related to identity-specific signals through functional connections between vmPFC and OFC. In the latter scenario, general value would be established independently of identity-specific representations [for example, through links with the

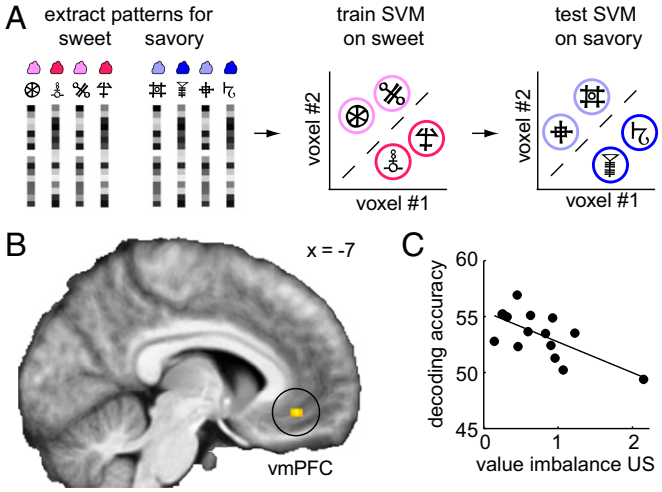


**Fig. 4.** vmPFC represents identity-general predictive values. (*A*) Schematic of the searchlight decoding analysis used to identify identity-independent value coding. SVM models were trained on activity patterns evoked by the CS images predicting the high- vs. low-value sweet odor and then, tested on patterns evoked by the CS predicting the high- vs. low-value savory odor (and vice versa). (*B*) Identity-general value in the vmPFC. Display threshold is $P < 0.001$. (*C*) Identity-general coding is higher when the imbalance between sweet and savory values is lower ($r = -0.68$, $P = 0.01$), further supporting the role of vmPFC in coding identity-general value.

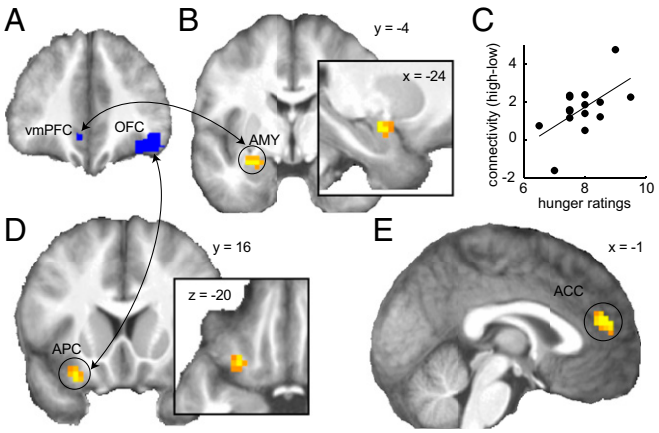


**Fig. 5.** Functional networks of general- and identity-specific value coding. (*A*) Seed regions used in the functional connectivity analyses. (*B*) Voxels in the amygdala (AMY) show a general value-related change in connectivity with vmPFC. (*C*) Individual differences in hunger significantly predict value-related connectivity between vmPFC and amygdala ($r = 0.58$, $P = 0.02$). (*D* and *E*) Regions in the (*D*) anterior piriform cortex (APC) and (*E*) ACC show identity-specific value-related connectivity with OFC. Display threshold is $P < 0.001$.

amygdala, which is involved in valuation and general affective processing (24, 25) and is strongly connected to vmPFC (26)]. To test these hypotheses, we used a psychophysiological interaction (PPI) model and searched for brain regions in which functional connectivity with vmPFC was modulated by general predictive value (high vs. low) collapsed across the two odor identities. Supporting the concept of an independent pathway, we found significant value-related connectivity changes between vmPFC and amygdala (−27, −4, −17; *t* test, $n = 15$; $t = 5.77$, $p_{FWE} = 0.003$) (Fig. 5*B*) but not OFC ($t = -1.25$, $P = 0.23$). Moreover, we found that subject-specific overall hunger ratings significantly predicted value-related vmPFC–amygdala connectivity ($r = 0.58$, $P = 0.02$) (Fig. 5*C*), showing that this connection is directly related to the general motivational value of the odors.

The finding that instantiation of general predictive value in vmPFC is not related to identity-specific value information in OFC aligns with observations that vmPFC and OFC reside in largely dissociable anatomical networks (27–29). In turn, we tested whether identity-specific value signals are functionally connected with olfactory cortices where odor identity is represented (30, 31). Using an SVM-based variation of PPI to identify brain regions where value-related OFC connectivity patterns differed between sweet vs. savory predicted odors, we found significant OFC connections with anterior piriform cortex (−27, 14, −20; *t* test, $n = 15$; $t = 4.08$, $p_{FWE} = 0.014$) (Fig. 5*D*) and ACC (−3, 47, 16; $t = 6.20$, $p_{FWE} = 0.011$) (Fig. 5*E*) but not vmPFC ($t = 0.87$, $P = 0.40$) or amygdala ($t = 1.83$, $P = 0.10$). These findings imply that identity-specific value signals in OFC are related to odor identity information in piriform cortex, a mechanism in keeping with the known bidirectional projections between these two brain areas (32).

## Discussion

To make adaptive choices, nervous systems must encode information about the identity of expected outcomes. Despite the importance of outcome-specific responding for adaptive and goal-directed behavior, most imaging research has focused on characterizing abstract value representations, while disregarding the specific identity of the reward (with a few exceptions) (4, 9). Here, we used appetizing food odors as rewards in an fMRI paradigm of human classical conditioning, enabling us to dissociate reward value and identity and examine neural representations of identity-specific value using pattern-based fMRI analyses. We found that identity-specific value codes in OFC and identity-general value codes in vmPFC were embedded in parallel functional networks involving primary sensory and limbic regions, respectively.

By applying SVM classifiers to value-related fMRI activity patterns associated with distinct reward identities (i.e., savory and sweet food odors), we found robust identity-specific value coding in a central/lateral region of the OFC. Although these results are seemingly at odds with the widely held idea that OFC signals a common currency for value or effect (3, 5, 8), one cannot claim equivalency in the strength of evidence between the failure to find a distributed general value signal using pattern-based fMRI and the finding of single-unit evidence for a common value code in monkey OFC (3). In fact, failure to detect such a code in fMRI does not preclude its existence at the single-unit level in either human or monkey OFC.

Nevertheless, our results indicate that predictive representations in the OFC conjointly signal both the identity and the value of the expected outcome in a unified neural code. At the level of single neurons, such a coding scheme could be implemented by units signaling both value and identity or an interaction between the two. Intriguingly, such neurons have recently been identified in the rat OFC (12), and it is likely that other features of the expected outcome, such as reward location, behavioral responses, and other valueless features, are also embedded in these complex predictive codes (3, 33–35). Thus, our findings indicate that predictive outcome representations in the OFC are much more complex than previously thought, and provide critical empirical support for recent proposals suggesting that the OFC plays a fundamental role in model-based behavior by tracking the contents and states of the environment and task structure (36, 37). Interestingly, identity-specific value signals were also identified in ACC and hippocampus. The potential functional relevance of these regions in predictive reward coding is described in *SI Discussion*.

In contrast to the identity-specific value codes found in OFC, identity-general value codes were found in the vmPFC. Here, patterns of fMRI activity coding for the predicted value of a sweet odor could be used to reliably classify the predicted value of a savory odor, and vice versa. This finding echoes and extends recent evidence showing that vmPFC activity patterns generalize across different reward categories (4, 5, 7), such as food items, merchandizing gimmicks, and leisure activities. In these studies, classifiers were trained on exemplars (i.e., different items) associated with different values in one category and could be used to predict the value of exemplars in another category. In contrast, here we manipulated value while keeping identity constant to show that value codes generalize across specific identities within a category, thereby providing a rigorous test for identity-independent value codes. However, rather than constituting a ubiquitous feature of the ventral prefrontal cortex, such coding was restricted to a localized portion of vmPFC. This observation is in line with previous reports (8), and accords with the idea that vmPFC is specialized to perform online evaluations of and comparisons between currently expected outcomes (38, 39). Arguably, if vmPFC neurons are, indeed, able to flexibly code the value of a wide range of stimuli, only a limited number of such neurons would be needed, which may account for why general value representations were confined to a relatively small area of vmPFC.

Strikingly, identity-specific and -general value signals revealed in this study were not serially related to each other but showed functional connections with a nonoverlapping set of brain regions. Whereas general value signals in vmPFC were linked to processing in the amygdala, identity-specific value codes in OFC were related to piriform cortex, an olfactory sensory region corresponding to the sensory modality of the rewards used in this study. This mechanism may highlight a fundamental principle, whereby identity-based sensory features of a reward are

extracted from sensory-relevant cortical areas, and then further processed in OFC to support the formation of identity-specific value codes. Supporting this model, lateral and posterior areas of OFC have been shown to receive direct projections from a wide range of sensory cortices (27, 40).

The embedding of identity-specific and -general value representations in parallel pathways alludes to a functional independence of these two signals. A general value code linked with the amygdala would support comparisons between different rewards (8) and map onto relatively coarse actions, such as approach or avoidance behaviors (2, 25). In contrast, an identity-specific pathway tied to sensory cortical representations would support more nuanced and differentiated behaviors (36), and thereby allow that prey is eaten and mates are courted—a differentiation that cannot be made using general value signals alone. Indeed, an inability to generate identity-specific value signals in OFC would have profound consequences for consummatory responses and lead directly to the types of pathological behaviors, including disinhibition, hyperorality, and hypersexuality, that are observed in patients with frontotemporal dementia or structural damage to limbic brain networks (41, 42). Our findings thus offer unique mechanistic insights and testable predictions that may help target future therapeutic interventions for these disorders.

## Materials and Methods

**Subjects.** Fifteen healthy subjects (seven males ages 23–29 years old, mean ± SD = 25.53 ± 2.33 years old) with normal or corrected-to-normal vision participated in the study. The study took place at the Northwestern University Feinberg School of Medicine according to protocols approved by the local Institutional Review Board.

**Experimental Design.** Subjects came into the laboratory on 3 consecutive days. On the first day, odor stimuli were selected, and subjects were trained on the conditioning task. On the second and third days, subjects performed 6 runs of an outcome prediction task inside the MRI scanner, resulting in a total of 12 runs. On all days, subjects were asked to fast for 6 h before the experiment. According to ratings of hunger provided on a scale from 1 (not at all hungry) to 10 (very hungry), subjects were sufficiently hungry on each day of testing (day 1 = 8 ± 0.28; day 2 = 7.8 ± 0.28; day 3 = 8 ± 0.22) and had not eaten for ∼6 h before the experiment (day 1 = 6.4 ± 0.95 h; day 2 = 5.9 ± 0.64 h; day 3 = 6.9 ± 1.03 h). *SI Materials and Methods* discusses details on odor stimulus selection, classical conditioning, and outcome prediction task as well as fMRI data acquisition and preprocessing.

**Odor Stimuli and Application.** Pleasant food odors (provided by International Flavors and Fragrances) were used as rewards in the experiment. Specifically, we used four sweet odors (cupcake, strawberry, dulce de leche, and watermelon) and four savory food odors (pizza, sautéed onions, potato chips, and barbecue sauce). For all experimental and rating tasks inside and outside the MRI scanner, odors were delivered directly to the nose of the subject using a custom-built, computer-controlled olfactometer according to previously established methods (20). The olfactometer was equipped with two independent mass flow controllers (Alicat) capable of precisely diluting up to 10 odorants with odorless air, such that we could change odor concentration (and thus, pleasantness) from trial to trial while maintaining perceptual identity.

**Multivoxel Pattern Analysis for Identity-Specific Value Codes.** To identify identity-specific value codes, we used a searchlight decoding approach (43–46) that allows information mapping without potentially biasing voxel selection (47) combined with linear kernel SVM. In a first step, we estimated a general linear model (GLM) on the realigned functional imaging data from each subject and each scanning run. The purpose of this GLM was to estimate the voxelwise value-related responses for each of two odors. Subsequently, these value-related responses were used to search for brain regions that differentially code the value of the two odors. The GLM contained four regressors (duration of 1.5 s) coding for the onset of the CS predicting sweet or savory odors separately for each CS set (regressor 1: CS from set I predicting high and low sweet; regressor 2: CS from set I predicting high and low savory; regressor 3: CS from set II predicting high and low sweet; regressor 4: CS from set II predicting high and low savory). These four onset regressors were each parametrically modulated by the value of the odor predicted by the CS (coded as 1 and −1 for high and low values). The GLM also included four regressors coding for the onsets of four different odor outcomes (sniffs to low and high sweet odors and low and high savory odors). All 12 regressors (4 CS onset, 4 CS value, and 4 US) were convolved with a canonical hemodynamic response function. The six movement parameters as well as two regressors accounting for parametric trial by trial fluctuations in sniff amplitude and sniff duration were included as nuisance regressors of no interest. The four parametric regressors from this GLM are orthogonalized to the corresponding CS onset regressor and thus, account for value-related variance separately for each odor identity and visual stimulus set (CS set I sweet, CS set I savory, CS set II sweet, and CS set II savory) independent of the variance related to expected odor identity. Thus, the voxelwise parameter estimates from these parametric regressors represent the value-related responses for the two different odors as signaled by two different stimulus sets.

In a second step, the parameter estimates from the parametric value regressors were used as input for an SVM decoding analysis to search for identity-specific value representations while controlling for the visual effects of the CS. The SVM was performed using the LIBSVM implementation (www.csie.ntu.edu.tw/~cjlin/libsvm/) with a linear kernel and a preselected cost parameter of $c = 0.01$. For each searchlight (all voxels within a radius of four voxels surrounding the central voxel) (45), we trained an SVM to classify value-related responses from sweet vs. savory expected odors as signaled by CS from set I and tested the SVM on value-related responses from sweet vs. savory expected odors as signaled by CS from set II. The procedure was repeated in the opposite direction by training on the sweet vs. savory value-related responses in CS set II and testing on sweet vs. savory value-related responses in CS set I. We also trained on sweet set I vs. savory set II and tested on sweet set II vs. savory set I and vice versa (reported results are averaged across all four directions). Importantly, decoding in this analysis can only be above chance if different multivoxel response patterns code the predicted value of the sweet and savory odor identities. Moreover, because we trained and tested the SVM on data from different CS sets, the results of this decoding analysis are independent of the visual features of the predictive CS.

**Multivoxel Pattern Analysis for Identity-Independent Value Codes.** To identify identity-independent value codes, we first set up a GLM to estimate response patterns for each unique CS. The GLM contained eight regressors for the onsets (duration of 1.5 s) of eight different CS (two sets of CS predicting low and high sweet odors and two sets of CS predicting low and high savory odors). The GLM also included four regressors coding for the onsets of four different odor outcomes and the nuisance regressors (sniff parameters and head motion) described above. The voxelwise parameter estimates of the first eight regressors represent the response amplitudes to each of eight CS predicting low and high sweet and savory food odors in each of 12 scanning runs.

In a second step, these eight parameter estimates were used as input for an SVM cross-identity decoding analysis to search for identity-independent value representations. For each searchlight, we trained an SVM on response patterns from CS predicting high vs. low sweet odors, and prediction accuracy was obtained by testing the SVM on response patterns from CS predicting high vs. low savory odors. The procedure was repeated in the opposite direction by training on the predicted value of the savory odors and testing on the predicted value of the sweet odors (reported results are averaged across both directions). All other parameters of the searchlight and the SVM were identical to the decoding analysis for identity-specific values described above. Importantly, this cross-identity decoding accuracy can only be significantly above chance if the same multivoxel response patterns code the predicted value of the sweet and the savory odors. Because sweet and savory odors are predicted by different visual CS, the results are independent of the visual features of the predictive CS.

**PPI Analysis.** We computed the general value-related functional connectivity of the vmPFC using a PPI analysis as implemented in the gPPI toolbox (48). Specifically, for each subject we estimated a PPI model with CS predicting high vs. low value as the psychological factor and seed activation of the vmPFC cluster identified in the identity-independent decoding analysis (defined at $P < 0.001$) as the physiological factor. The model also included regressors coding for the onsets of the CS and US, as well as the sniff and head motion parameters (described above) as nuisance variables of no interest. Individual contrast images for general value-dependent (high vs. low) connectivity changes with the vmPFC were computed and subjected to voxelwise group-level analyses.

**Multivoxel PPI Analysis.** To reveal brain regions that show identity-specific value-related connectivity with the OFC, a pattern-based connectivity method was required, because no univariate differences in value-related connectivity were expected between the two predicted odor identities (because of the distributed nature of odor coding) (30, 31). Accordingly, we combined the PPI analysis with the multivoxel pattern analysis described

above (*Multivoxel Pattern Analysis for Identity-Specific Value Codes*). In a first step, for each scanning run, we estimated a PPI model for value-related connectivity as described above (*PPI Analysis*) using the OFC (cluster defined at $P < 0.001$ from the identity-specific decoding analysis) as a seed region. In this model, however, we computed the value-related connectivity estimates separately for CS predicting sweet and savory odors. In a second step, we used these identity-specific value-related connectivity estimates as input to a leave one run out cross-validated SVM searchlight analysis to identify brain regions that show different value-related connectivity patterns with the OFC for sweet vs. savory predicted odors. Specifically, instead of using the value-related response amplitudes for different predicted odors to train the SVM (as used in the identity-specific decoding analysis described above), here, we used the voxelwise sweet and savory value-related OFC connectivity estimates to search for brain regions where predicted odor identity could be decoded based on OFC connectivity patterns.

**Group-Level Analysis.** To test for significant identity-specific and -general value coding, we performed group-level analyses ($n = 15$ subjects) by using voxelwise one-sample *t* tests on smoothed accuracy maps (6-mm FWHM). All group-level analyses were carried out in an explicit anatomical mask comprising the OFC, ACC, insula, anterior and posterior piriform cortex, amygdala, and hippocampus.

To control for relative value differences between odor identities across subjects, all group-level analyses included the value imbalance score (*SI Materials and Methods*) for CS and US ratings as covariates of no interest. The same tests were used to identify regions showing functional connectivity with the vmPFC and OFC. We applied a statistical threshold of $P < 0.05$ corrected for multiple comparisons (FWE). Based on a priori hypotheses regarding encoding of identity-general and -specific values, correction was performed for the following anatomical regions of interest from the automated anatomical labeling atlas: OFC (superior orbital gyrus, middle orbital gyrus, and inferior orbital gyrus), vmPFC (gyrus rectus and medial orbital gyrus), ACC, anterior piriform cortex, amygdala, and hippocampus. For display purposes, all imaging results are presented at $P < 0.001$ (uncorrected).

**ACKNOWLEDGMENTS.** Special thanks to International Flavors and Fragrances (S. Miller and S. Warrenburg) for providing food odorants, and Sydni Cole for assistance in acquiring the fMRI data. This work was supported by National Institute on Deafness and Other Communication Disorders Grants 1F31DC013500 (to J.D.H.) and R01DC010014 (to J.A.G.), National Institute of Neurological Disorders and Stroke Grant T32NS047987 (to J.D.H.), and Swiss National Science Foundation Grants PP00P1_128574 (to P.N.T.), PP00P1_150739 (to P.N.T.), and CRSII3_141965 (to P.N.T.).

1. Schleyer M, Miura D, Tanimura T, Gerber B (2015) Learning the specific quality of taste reinforcement in larval Drosophila. *eLife* 4:4.
2. Morrison SE, Salzman CD (2009) The convergence of information about rewarding and aversive stimuli in single neurons. *J Neurosci* 29(37):11471–11483.
3. Padoa-Schioppa C, Assad JA (2006) Neurons in the orbitofrontal cortex encode economic value. *Nature* 441(7090):223–226.
4. McNamee D, Rangel A, O'Doherty JP (2013) Category-dependent and category-independent goal-value codes in human ventromedial prefrontal cortex. *Nat Neurosci* 16(4):479–485.
5. Chikazoe J, Lee DH, Kriegeskorte N, Anderson AK (2014) Population coding of affect across stimuli, modalities and individuals. *Nat Neurosci* 17(8):1114–1122.
6. Kable JW, Glimcher PW (2009) The neurobiology of decision: Consensus and controversy. *Neuron* 63(6):733–745.
7. Gross J, et al. (2014) Value signals in the prefrontal cortex predict individual preferences across reward categories. *J Neurosci* 34(22):7580–7586.
8. Levy DJ, Glimcher PW (2012) The root of all value: A neural common currency for choice. *Curr Opin Neurobiol* 22(6):1027–1038.
9. Klein-Flügge MC, Barron HC, Brodersen KH, Dolan RJ, Behrens TE (2013) Segregated encoding of reward-identity and stimulus-reward associations in human orbitofrontal cortex. *J Neurosci* 33(7):3202–3211.
10. Rudebeck PH, Murray EA (2014) The orbitofrontal oracle: Cortical mechanisms for the prediction and evaluation of specific behavioral outcomes. *Neuron* 84(6):1143–1156.
11. Sescousse G, Redouté J, Dreher JC (2010) The architecture of reward value coding in the human orbitofrontal cortex. *J Neurosci* 30(39):13095–13104.
12. Stalnaker TA, et al. (2014) Orbitofrontal neurons infer the value and identity of predicted outcomes. *Nat Commun* 5:3926.
13. Burke KA, Franz TM, Miller DN, Schoenbaum G (2008) The role of the orbitofrontal cortex in the pursuit of happiness and more specific rewards. *Nature* 454(7202):340–344.
14. McDannald MA, et al. (2014) Orbitofrontal neurons acquire responses to 'valueless' Pavlovian cues during unblocking. *Elife* 3(2014):e02653.
15. Gottfried JA, O'Doherty J, Dolan RJ (2003) Encoding predictive reward value in human amygdala and orbitofrontal cortex. *Science* 301(5636):1104–1107.
16. Small DM, Veldhuizen MG, Felsted J, Mak YE, McGlone F (2008) Separable substrates for anticipatory and consummatory food chemosensation. *Neuron* 57(5):786–797.
17. O'Doherty J, et al. (2000) Sensory-specific satiety-related olfactory activation of the human orbitofrontal cortex. *Neuroreport* 11(4):893–897.
18. Moskowitz HR, Dravnieks A, Klarman LA (1976) Odor intensity and pleasantness for a diverse set of odorants. *Percept Psychophys* 19(2):122–128.
19. Gottfried JA, Dolan RJ (2004) Human orbitofrontal cortex mediates extinction learning while accessing conditioned representations of value. *Nat Neurosci* 7(10):1144–1152.
20. Gottfried JA, Deichmann R, Winston JS, Dolan RJ (2002) Functional heterogeneity in human olfactory cortex: An event-related functional magnetic resonance imaging study. *J Neurosci* 22(24):10819–10828.
21. Kahnt T, Park SQ, Haynes JD, Tobler PN (2014) Disentangling neural representations of value and salience in the human brain. *Proc Natl Acad Sci USA* 111(13):5000–5005.
22. Ongür D, Ferry AT, Price JL (2003) Architectonic subdivision of the human orbital and medial prefrontal cortex. *J Comp Neurol* 460(3):425–449.
23. Mackey S, Petrides M (2010) Quantitative demonstration of comparable architectonic areas within the ventromedial and lateral orbital frontal cortex in the human and the macaque monkey brains. *Eur J Neurosci* 32(11):1940–1950.
24. Baxter MG, Murray EA (2002) The amygdala and reward. *Nat Rev Neurosci* 3(7):563–573.
25. Paton JJ, Belova MA, Morrison SE, Salzman CD (2006) The primate amygdala represents the positive and negative value of visual stimuli during learning. *Nature* 439(7078):865–870.
26. Amaral DG, Price JL (1984) Amygdalo-cortical projections in the monkey (Macaca fascicularis). *J Comp Neurol* 230(4):465–496.
27. Carmichael ST, Price JL (1996) Connectional networks within the orbital and medial prefrontal cortex of macaque monkeys. *J Comp Neurol* 371(2):179–207.
28. Zald DH, et al. (2014) Meta-analytic connectivity modeling reveals differential functional connectivity of the medial and lateral orbitofrontal cortex. *Cereb Cortex* 24(1):232–248.
29. Kahnt T, Chang LJ, Park SQ, Heinzle J, Haynes JD (2012) Connectivity-based parcellation of the human orbitofrontal cortex. *J Neurosci* 32(18):6240–6250.
30. Howard JD, Plailly J, Grueschow M, Haynes JD, Gottfried JA (2009) Odor quality coding and categorization in human posterior piriform cortex. *Nat Neurosci* 12(7):932–938.
31. Zelano C, Mohanty A, Gottfried JA (2011) Olfactory predictive codes and stimulus templates in piriform cortex. *Neuron* 72(1):178–187.
32. Carmichael ST, Clugnet MC, Price JL (1994) Central olfactory connections in the macaque monkey. *J Comp Neurol* 346(3):403–434.
33. Furuyashiki T, Holland PC, Gallagher M (2008) Rat orbitofrontal cortex separately encodes response and outcome information during performance of goal-directed behavior. *J Neurosci* 28(19):5127–5138.
34. Feierstein CE, Quirk MC, Uchida N, Sosulski DL, Mainen ZF (2006) Representation of spatial goals in rat orbitofrontal cortex. *Neuron* 51(4):495–507.
35. Kennerley SW, Behrens TE, Wallis JD (2011) Double dissociation of value computations in orbitofrontal and anterior cingulate neurons. *Nat Neurosci* 14(12):1581–1589.
36. Jones JL, et al. (2012) Orbitofrontal cortex supports behavior and learning using inferred but not cached values. *Science* 338(6109):953–956.
37. Wilson RC, Takahashi YK, Schoenbaum G, Niv Y (2014) Orbitofrontal cortex as a cognitive map of task space. *Neuron* 81(2):267–279.
38. Strait CE, Blanchard TC, Hayden BY (2014) Reward value comparison via mutual inhibition in ventromedial prefrontal cortex. *Neuron* 82(6):1357–1366.
39. Barron HC, Dolan RJ, Behrens TE (2013) Online evaluation of novel choices by simultaneous representation of multiple memories. *Nat Neurosci* 16(10):1492–1498.
40. Cavada C, Compañy T, Tejedor J, Cruz-Rizzolo RJ, Reinoso-Suárez F (2000) The anatomical connections of the macaque monkey orbitofrontal cortex. A review. *Cereb Cortex* 10(3):220–242.
41. Woolley JD, et al. (2007) Binge eating is associated with right orbitofrontal-insular-striatal atrophy in frontotemporal dementia. *Neurology* 69(14):1424–1433.
42. Miller BL, Cummings JL, McIntyre H, Ebers G, Grode M (1986) Hypersexuality or altered sexual preference following brain injury. *J Neurol Neurosurg Psychiatry* 49(8):867–873.
43. Kriegeskorte N, Goebel R, Bandettini P (2006) Information-based functional brain mapping. *Proc Natl Acad Sci USA* 103(10):3863–3868.
44. Kahnt T, Heinzle J, Park SQ, Haynes JD (2011) Decoding the formation of reward predictions across learning. *J Neurosci* 31(41):14624–14630.
45. Kahnt T, Heinzle J, Park SQ, Haynes JD (2010) The neural code of reward anticipation in human orbitofrontal cortex. *Proc Natl Acad Sci USA* 107(13):6010–6015.
46. Haynes JD, et al. (2007) Reading hidden intentions in the human brain. *Curr Biol* 17(4):323–328.
47. Kriegeskorte N, Simmons WK, Bellgowan PS, Baker CI (2009) Circular analysis in systems neuroscience: The dangers of double dipping. *Nat Neurosci* 12(5):535–540.
48. McLaren DG, Ries ML, Xu G, Johnson SC (2012) A generalized form of context-dependent psychophysiological interactions (gPPI): A comparison to standard approaches. *Neuroimage* 61(4):1277–1286.